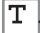



Page Proof Instructions and Queries

Journal Title: Journal of Cerebral Blood Flow & Metabolism (JCB)

Article Number: 780602

Thank you for choosing to publish with us. This is your final opportunity to ensure your article will be accurate at publication. Please review your proof carefully and respond to the queries using the circled tools in the image below, which are available by clicking “Comment” from the right-side menu in Adobe Reader DC.*

Please use *only* the tools circled in the image, as edits via other tools/methods can be lost during file conversion. For comments, questions, or formatting requests, please use  Please do *not* use comment bubbles/sticky notes .



*If you do not see these tools, please ensure you have opened this file with Adobe Reader DC, available for free at get.adobe.com/reader or by going to Help > Check for Updates within other versions of Reader. For more detailed instructions, please see us.sagepub.com/ReaderXProofs.

| No. | Query |
|-------|--|
| | Please confirm that all author information, including names, affiliations, sequence, and contact details, is correct. |
| | Please review the entire document for typographical errors, mathematical errors, and any other necessary corrections; check headings, tables, and figures. |
| | Please confirm that the Funding and Conflict of Interest statements are accurate. |
| | Please ensure that you have obtained and enclosed all necessary permissions for the reproduction of artistic works, (e.g. illustrations, photographs, charts, maps, other visual material, etc.) not owned by yourself. Please refer to your publishing agreement for further information. |
| | Please note that this proof represents your final opportunity to review your article prior to publication, so please do send all of your changes now. |
| AQ: 1 | The reference ‘Buxton et al., 1998’ does not seem to be listed in the reference list. Kindly include (in which case, please include the appropriate number in the citation and remove the year, as this journal follows numbered reference style) or delete the text citation. |
| AQ: 2 | Please check clarity: ‘...of systemic arterial hypertension, ¹¹ and the phenotype is consistent with the role of...’ |
| AQ: 3 | Please provide the place where the conference was held, date–month of the conference, page range and location of the publisher in Ref. 21. |
| AQ: 4 | Please provide the location of the publisher in Ref. 22. |
| AQ: 5 | Please provide the location of the publisher in Ref. 24. |
| AQ: 6 | Please provide the volume number and page range in Ref. 29. |

A critical role for the ATP-sensitive potassium channel subunit $K_{IR6.1}$ in the control of cerebral blood flow

Patrick S Hosford^{1,2}, Isabel N Christie^{2,3}, Arun Niranjana³, Qadeer Aziz¹, Naomi Anderson¹, Richard Ang², Mark F Lythgoe³, Jack A Wells³, Andrew Tinker¹ and Alexander V Gourine²

Abstract

$K_{IR6.1}$ (KCNJ8) is a subunit of ATP sensitive potassium channel (K_{ATP}) that plays an important role in the control of peripheral vascular tone and is highly expressed in brain contractile cells (vascular smooth muscle cells and pericytes). This study determined the effect of global deletion of the $K_{IR6.1}$ subunit on cerebral blood flow, neurovascular coupling and cerebral oxygenation in mice. In $K_{IR6.1}$ deficient mice resting cerebral blood flow and brain parenchymal partial pressure of oxygen (PO_2) were found to be markedly lower compared to that in their wildtype littermates. However, cortical blood oxygen level dependent responses triggered by visual stimuli were not affected in conditions of $K_{IR6.1}$ deficiency. These data suggest that K_{ATP} channels containing $K_{IR6.1}$ subunit are critically important for the maintenance of normal cerebral perfusion and parenchymal PO_2 but play no significant role in the mechanisms underlying functional changes in brain blood flow.

Keywords

Cerebral blood flow, cerebrovascular reactivity, functional magnetic resonance imaging, hypoxia, neurovascular coupling

Received 21 July 2017; Revised 20 April 2018; Accepted 1 May 2018

Introduction

Neurovascular coupling dynamically regulates the blood supply to active brain areas to match metabolic demand and supply.¹ In pathological conditions, including Alzheimer's disease,² hypertension,³ stroke,⁴ traumatic brain injury⁵ and glioma,⁶ compromised cerebral blood flow (CBF) may contribute to the development and/or progression of the disease, highlighting the importance of understanding the mechanisms controlling resting and dynamic CBF.

Ion channels that determine the membrane potential of cerebrovascular smooth muscle cells (potassium channels for example) are likely to be important for the control of CBF (for review see Longden et al.⁷). Even small increases in extracellular potassium can have a profound effect on vascular tone by activating inwardly rectifying potassium channels expressed in the vascular smooth muscle cells.^{8,9} Recent data suggest that $K_{IR2.1}$ potassium channels mediate the effect of

increased extracellular K^+ on cerebral vasculature and contribute to the operation of mechanisms underlying increases in local CBF which follow changes in neuronal activity.¹⁰

Another notable family of K^+ channels include ATP-sensitive potassium channels (K_{ATP}). In the periphery, $K_{IR6.1}$ plays an important role in determining resting vascular tone, peripheral resistance and,

¹William Harvey Research Institute, Barts and the London School of Medicine and Dentistry, London, UK

²Centre for Cardiovascular and Metabolic Neuroscience, Neuroscience, Physiology & Pharmacology, University College London, London, UK

³UCL Centre for Advanced Biomedical Imaging, Division of Medicine, University College London, London, UK

Corresponding author:

Alexander V Gourine, Centre for Cardiovascular and Metabolic Neuroscience, Neuroscience, Physiology & Pharmacology, University College London, Gower Street, London WC1E 6BT, UK.
Email: a.gourine@ucl.ac.uk

therefore, systemic arterial blood pressure. Global $K_{IR6.1}$ deficiency in an animal (mouse) model was reported to be associated with chronically elevated (by ~ 20 mmHg) systemic arterial blood pressure.¹¹ In the brain, drugs which promote opening of K_{ATP} channels were reported to induce dilations of basilar and middle cerebral arteries in a rat model.¹²

$K_{IR6.1}$ is also abundantly expressed by brain pericytes and was previously suggested to be used as a molecular marker of this cell type.¹³ Evidence is accumulating that these contractile cells play a critical role in neurovascular coupling,^{14,15} although this idea has been disputed.^{16,17} K_{ATP} channel activation hyperpolarises pericytes as demonstrated in retinal microvasculature.¹⁸ As K_{ATP} channels are sensitive to changes in intracellular concentrations of ATP/ADP, this positions $K_{IR6.1}$ as a possible metabolic sensor of pericytes.

In this study, we determined the effect of global deletion of the $K_{IR6.1}$ channel on resting CBF, cerebrovascular reactivity to CO_2 , neurovascular coupling and brain tissue PO_2 in mice. The data obtained suggest that $K_{IR6.1}$ is critically important for the maintenance of normal cerebral perfusion and oxygenation but plays no significant role in the generation of blood oxygen level dependent (BOLD) responses to sensory stimulation.

Materials and methods

Animals

The experiments were performed on 35 male mice (two to three months old) in accordance with the European Commission Directive 86/609/EEC (European Convention for the Protection of Vertebrate Animals used for Experimental and Other Scientific Purposes) and the United Kingdom Home Office (Scientific Procedures) Act (1986) with project approval from the Institutional Animal Care and Use Committee. The results of the animal experimentations are reported in accordance with ARRIVE guidelines.

Generation of the $K_{IR6.1}$ knockout mouse strain has been previously described in detail.¹¹ Briefly, crossing homozygous $K_{IR6.1}$ floxed mice with a mouse ubiquitously expressing Cre recombinase on a C57Bl/6 background produced mice with global deletion of one allele of $K_{IR6.1}$. The progeny were then backcrossed onto a C57Bl/6 background for at least six generations. Resulting $K_{IR6.1}^{+/-}$ mice were then crossed to produce homozygotes.

The animals were housed in a temperature controlled room at $21 \pm 2^\circ C$ and a relative humidity of $55 \pm 10\%$, with a 12-h light/12-h dark cycle with a 30 min twilight period.

fMRI and analysis

All MRI experiments were performed using a 9.4T MRI scanner (Agilent Inc.), a 72 mm inner diameter volume coil for radio frequency transmission (Rapid Biomedical) and a 2-channel array surface coil (Rapid Biomedical) for signal reception.

The animals were anaesthetised with isoflurane (4–5% in O_2) and placed in the scanner bore. Medetomidine (0.4 mg kg^{-1} bolus, followed by infusion $0.8 \text{ mg kg}^{-1} \text{ h}^{-1}$, s.c.) was administered to induce and maintain deep sedation for the duration of the experiment. Isoflurane was discontinued and the mice were free breathing with body temperature maintained at $37 \pm 1^\circ C$ using a servo-controlled heating blanket. A nose cone was used to deliver oxygen enriched ($\sim 30\%$) air and to apply CO_2 challenges. To stimulate visual sensory pathways, 2 Hz pulses of cold white light were delivered to the scanner bore so that light reflected off the surface of the head coil stimulated the eyes with diffuse light. The stimulus was delivered using a block design paradigm of 40 s rest, 20 s activation, repeated three times.

Arterial spin labelling (ASL) was used to measure CBF at rest and during systemic hypercapnia. Baseline cerebral perfusion in the cortex was mapped using a flow sensitive alternating inversion recovery sequence with a three shot segmented gradient echo EPI readout (TE = 5.8 ms, TR = 5 s, TI = 2 s, 3 slices, 1 mm slice thickness). Repeated ASL images (acquired every 30 s) were captured for 10 min at baseline conditions, during 5 min of CO_2 challenge (5% CO_2 in the inspired gas mixture), and during a 3.5 min period of recovery. This experimental protocol was repeated three times for each the animal. Maps of CBF were generated by fitting the data to the established model (Buxton et al., 1998). The mean CBF within the cortex was plotted from manually drawn regions of interest (ROI). **AQ1**

The fMRI methods used in this study were described in detail elsewhere.^{19,20} Briefly, anatomical reference scans were acquired using a fast spin echo sequence (TR/TE_{eff} = 4000/48 ms, ETL = 8, matrix size = 192×192 , FOV = $35 \times 35 \text{ mm}^2$, 35 coronal slices each 0.6 mm thick). Functional data were acquired using four snapshot GE-EPI sequence (FOV = $35 \times 35 \text{ mm}^2$, matrix size = 96×96 , 12 coronal slices each 0.5 mm thick, slice gap 0.1 mm, spectral width = 178.6 kHz, TR = 2.5 s, TE = 19 ms, 131 volumes including one triple reference scan, total scan time approximately 5.5 min). Each subject underwent one anatomical reference scan and two fMRI scans.

Acquired fMRI data were analysed offline using NiftyReg,²¹ in-house MATLAB 2013a scripts and SPM12,²² as previously described.²⁰ Brain anatomical reference images were registered to the Allen Mouse

Brain Atlas²³ using an affine registration via an MRI template. Each affine transformation matrix was then applied to the individual fMRI data to normalise each subject into the atlas space. The registration was evaluated by visual inspection using SPM12 and the Mouse Brain Atlas.²⁴ After registration, the fMRI data were realigned, corrected for differences in slice timing and smoothed (Gaussian FWHM of two voxels).

Scans were screened for artefacts (gross motion, Nyquist ghosting and signal drop-out due to B_0 field inhomogeneities) by visual inspection performed by the investigator blinded to the nature of the experimental group. After screening, three subjects were excluded from the analysis (two $K_{IR6.1}$ knockout and one wildtype mice), giving final group sizes indicated in Figure 1. ROI-based analysis was conducted by using

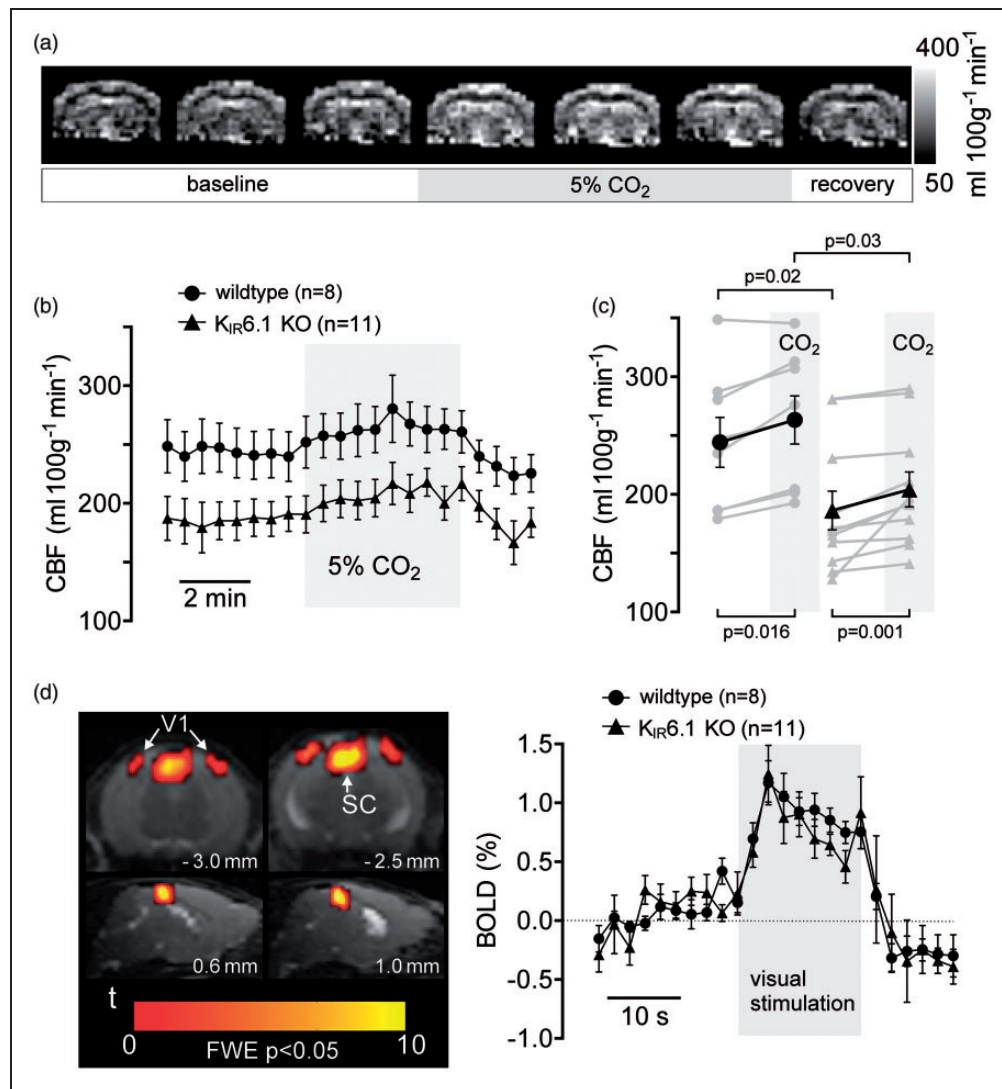


Figure 1. Resting cerebral blood flow (CBF), cerebrovascular reactivity to CO₂, and blood oxygen level dependent (BOLD) fMRI responses in the visual cortex in mice lacking K_{ATP} channel subunit K_{IR6.1}. (a) Representative arterial spin labelling brain maps illustrating measurements of CBF at baseline, during CO₂ challenge (5% CO₂ in the inspired gas mixture) and following recovery in a K_{IR6.1} knockout (KO) mouse (7 CBF maps of the total time series of 22 are shown); (b) Mean time-course of the whole brain CBF determined using arterial spin labelling MRI in K_{IR6.1} knockout and wildtype mice at resting conditions and in response to CO₂ challenge; (c) Summary data illustrating resting CBF and peak increases in CBF in response to CO₂ in K_{IR6.1} deficient and wildtype mice; (d) Representative BOLD activation maps (FWE, familywise error, $P < 0.05$, $n_v = 3$) taken at two coronal (top, distance from Bregma is indicated) and two sagittal (bottom, distance from the midline is indicated) levels showing activation of visual pathways in the brain of a K_{IR6.1} knockout mouse and BOLD response curves illustrating changes in mean signal within the primary visual cortex (V1) induced by visual stimulation (20s) in K_{IR6.1} knockout and wildtype mice. SC: superior colliculus. Data are presented as individual values and/or means \pm SEM.

MRI atlas labels to determine time courses using the MarsBaR toolbox. Bilateral ROIs were chosen for timecourse extraction within V1 of the mouse visual cortex (region code VISp in the Allen Mouse Brain Atlas). BOLD signals were calculated by subtracting the mean baseline value from the mean BOLD values acquired during each stimulation epoch. All experiments were performed blindly and all the analyses were done by individuals blinded to the nature of the experimental groups.

Brain parenchymal PO_2 measurements

Anaesthesia was induced and maintained with isoflurane (5% induction, 2–3% maintenance). Core temperature was kept at $\sim 37^\circ\text{C}$ using a heating blanket. Carotid artery was cannulated to record systemic arterial blood pressure. The animal was placed in a stereotaxic frame and the skull was exposed. A small hole was drilled in the parietal bone above the primary visual cortex (V1) using the following coordinates: 1.0 mm rostral to lambda and 2.5 mm lateral from the midline. The dura was punctured and an OxyliteTM optical oxygen sensor (Oxford Optronix) was lowered into the cortical tissue to a depth of ~ 1 mm from the surface of the brain. The craniotomy was then sealed with a layer of petroleum jelly to prevent diffusion of ambient oxygen. Parenchymal PO_2 sampling continued for 10 min until a stable reading was achieved. PO_2 , PCO_2 and pH of the arterial blood were measured using a Siemens blood gas analyser (RapidLab 248). Data were analysed off-line using *Spike 2* software (Cambridge Electronic Design).

Statistics

Differences in grouped mean data were tested for significance using Wilcoxon's signed rank test or Mann–Whitney test, where appropriate. Differences with $p < 0.05$ were considered to be significant

Results

ASL method was first used to quantify CBF in the wildtype and $K_{IR6.1}$ deficient mice (Figure 1(a) to (c)). Resting CBF was found to be lower in $K_{IR6.1}$ knockout animals compared to that recorded in their wildtype littermates (186 ± 16 vs. 244 ± 21 ml $100\text{ g}^{-1}\text{ min}^{-1}$; $p = 0.02$). However, CBF CO_2 responses were not affected in conditions of $K_{IR6.1}$ deficiency. In response to a CO_2 challenge (5% inspired CO_2 ; 5 min; increase in the arterial PCO_2 from 44 ± 3 to 66 ± 3 mmHg), CBF increased from 244 ± 21 to 263 ± 21 ml $100\text{ g}^{-1}\text{ min}^{-1}$ in wildtype animals (0.35% ΔCBF per mmHg arterial PCO_2) and from 186 ± 16 to 203 ± 15 ml $100\text{ g}^{-1}\text{ min}^{-1}$

in $K_{IR6.1}$ knockout mice (0.44% ΔCBF per mmHg arterial PCO_2). Thus, although resting CBF was significantly lower in $K_{IR6.1}$ knockout animals, there was no difference in the magnitude of CO_2 -induced cerebrovascular responses between the groups (CBF increased by 19.0 ± 5 vs. 17.8 ± 6 ml $100\text{ g}^{-1}\text{ min}^{-1}$ in the wildtype and $K_{IR6.1}$ knockout mice, respectively; $p = 0.438$) (Figure 1(c)).

Sensory-evoked BOLD functional magnetic resonance imaging (fMRI) responses were next assessed in the primary visual cortex of $K_{IR6.1}$ knockout mice and their wildtype counterparts (Figure 1(d)). The time course data show that the magnitude and profile of cortical BOLD responses triggered by visual stimuli were not affected in conditions of $K_{IR6.1}$ deficiency. Peak BOLD responses were $1.2 \pm 0.6\%$ Δ in the wildtype mice and $1.3 \pm 0.4\%$ Δ in $K_{IR6.1}$ knockout mice (Figure 1(d)).

Due to the recorded differences in resting CBF between the wildtype and $K_{IR6.1}$ deficient mice (Figure 1(b) and (c)), we next determined whether reduced cerebral perfusion is associated with altered brain tissue PO_2 . Parenchymal PO_2 was measured in the visual cortex in animals' breathing room air under isoflurane anaesthesia. Mean systemic arterial blood pressure was found to be significantly higher in $K_{IR6.1}$ knockout animals compared to that in wildtype mice (85 ± 6 vs. 70 ± 2 mmHg; $p = 0.04$) (Figure 2(a)), confirming data obtained in conscious $K_{IR6.1}$ deficient mice.¹¹ Although, the arterial blood pressure was higher, $K_{IR6.1}$ knockout animals were found to have a significantly lower brain parenchymal PO_2 than their wildtype counterparts (23.3 ± 6.4 vs. 45.1 ± 4.0 mmHg; $p = 0.035$) (Figure 2(b)). There were no differences in the arterial PO_2 , PCO_2 and pH (7.34 ± 0.03 , $n = 6$ vs. 7.38 ± 0.04 , $n = 6$; $p = 0.9$) between $K_{IR6.1}$ deficient and wildtype mice (Figure 2(c) to (d)).

Discussion

In this study, we tested the hypothesis that K_{ATP} channels containing the $K_{IR6.1}$ subunit (highly expressed by vascular smooth muscle cells and pericytes) maintain cerebrovascular tone and, therefore, play an important role in the control of CBF. The data obtained demonstrate that $K_{IR6.1}$ deficiency in mice is associated with a significant reduction in basal CBF and brain tissue PO_2 , despite normal level of arterial oxygenation and higher systemic arterial blood pressure. Cerebrovascular reactivity to CO_2 and sensory-evoked BOLD fMRI responses in the visual cortex (a measure of neurovascular coupling) were not affected in conditions of $K_{IR6.1}$ deficiency.

Central to our original hypothesis, $K_{IR6.1}$ channel activity can be modulated by various metabolic signals

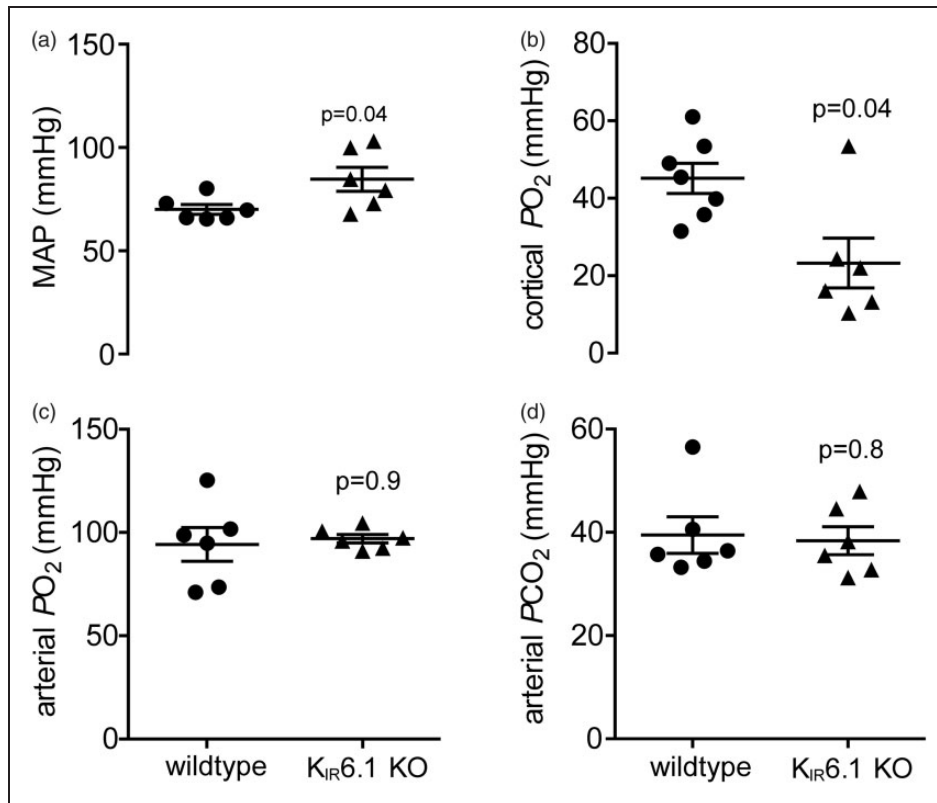


Figure 2. Reduced parenchymal partial pressure of oxygen (PO_2) in the visual cortex in mice lacking K_{ATP} channel subunit $K_{IR6.1}$. Summary data illustrating mean arterial blood pressure (MAP) (a) resting brain tissue PO_2 (b), arterial PO_2 (c), and arterial PCO_2 (d) in $K_{IR6.1}$ knockout (KO) and wildtype mice. Data are presented as individual values and means \pm SEM.

(such as increased energy demand or changes in pH) and, therefore, play a certain role in the mechanisms underlying cerebrovascular responses to increased neuronal activity.^{25,26} This hypothesis was supported by the evidence of strong $K_{IR6.1}$ subunit expression in the arterial smooth muscle cells and brain pericytes.¹³ Despite high expression of $K_{IR6.1}$ in contractile brain cells that regulate cerebrovascular tone and the molecular properties of $K_{IR6.1}$ underlying detection and integration of metabolic signals, this channel appears to be dispensable for neurovascular coupling (as measured by the BOLD response).

Although $K_{IR6.1}$ channel activity is sensitive to pH,²⁵ $K_{IR6.1}$ deletion had no effect on cerebrovascular reactivity to CO_2 , suggesting that this ATP and H^+ sensitive channel is not involved in dynamic regulation of CBF. However, a significant limitation in interpretation of these results is that cerebrovascular responses to CO_2 recorded in both $K_{IR6.1}$ deficient and wildtype mice were markedly smaller compared to typical cerebrovascular CO_2 reactivity of 2–4% Δ CBF change per mmHg of arterial PCO_2 reported in other published studies, including data obtained by our group in isoflurane-anaesthetized mice.²⁷ In the current study, ASL was performed under medetomidine sedation, which is

the latest popular sedative for rodents in fMRI experiments. As hypercapnic challenge led to significant increases in the arterial PCO_2 , these data suggest that medetomidine may impair cerebrovascular reactivity. Although identical experimental protocols were applied to knockout and wildtype mice and similar absolute increases in CBF during hypercapnia in these two cohorts were recorded, we cannot exclude that $K_{IR6.1}$ channels contribute to cerebrovascular CO_2 reactivity in an unanaesthetized state or when studied using anaesthetics other than medetomidine.

Our data provide the first evidence that K_{ATP} channel activity is critically important for the control of basal CBF. $K_{IR6.1}$ involvement in the control of brain perfusion is likely to be exerted at the level of cerebral supply vessels. This hypothesis is supported by the evidence that compounds which promote opening of K_{ATP} channels induce dilations of basilar and middle cerebral arteries.¹² There is also evidence that pharmacological blockade of K_{ATP} channels can trigger constrictions of some cerebral vessels, including dural²⁸ and middle meningeal arteries.²⁹

[AQ2] An earlier study reported that in mice global $K_{IR6.1}$ deficiency is leading to the development of systemic arterial hypertension,¹¹ and the phenotype is

consistent with the role of this channel in determining peripheral vascular tone. However, there is evidence that brain hypoxia may contribute to the development of systemic hypertension by the recruitment of the brainstem hypoxia-sensitive mechanism, mediated by astrocytes,³⁰ leading to enhanced central sympathetic drive.³¹ It is possible that reduced cerebrovascular flow and brain hypoxia observed in $K_{IR6.1}$ deficient animals contribute to the development of hypertensive phenotype in this model.

In summary, the data obtained in the present study suggest that $K_{IR6.1}$ is critically important for the maintenance of normal cerebral perfusion and brain tissue PO_2 , which ensures brain longevity. $K_{IR6.1}$ appears to be dispensable for functional dynamic changes in CBF.

Funding

The author(s) disclosed receipt of the following financial support for the research, authorship, and/or publication of this article: This work was supported by The Wellcome Trust (AVG), British Heart Foundation (RG/15/15/31742 to AT) and The National Institute for Health Research Barts Cardiovascular Biomedical Research Unit. AVG is a Wellcome Trust Senior Research Fellow (Refs: 095064 and 200893). ML receives funding from the EPSRC (EP/N034864/1); the King's College London and UCL Comprehensive Cancer Imaging Centre CR-UK & EPSRC, in association with the MRC and DoH (England); UK Regenerative Medicine Platform Safety Hub (MRC: MR/K026739/1); Eli Lilly and Company.

Declaration of conflicting interests

The author(s) declared no potential conflicts of interest with respect to the research, authorship, and/or publication of this article.

Authors' contributions

AVG, PSH and JAW designed research; PSH, INC, AN, JAW, QA, NA, and RA performed research; MFL and AT contributed unpublished reagents/analytic tools; PSH, INC, AN and JAW analysed data; PSH, IC, and AVG wrote the paper; all authors revised the article critically for important intellectual content.

References

1. Attwell D, Buchan AM, Charpak S, et al. Glial and neuronal control of brain blood flow. *Nature* 2010; 468: 232–243.
2. Lourenco CF, Ledo A, Dias C, et al. Neurovascular and neurometabolic derailment in aging and Alzheimer's disease. *Front Aging Neurosci* 2015; 7: 103.
3. Calcinaghi N, Wyss MT, Jolivet R, et al. Multimodal imaging in rats reveals impaired neurovascular coupling in sustained hypertension. *Stroke* 2013; 44: 1957–1964.
4. Prunell GF, Mathiesen T and Svendgaard NA. Experimental subarachnoid hemorrhage: cerebral blood flow and brain metabolism during the acute phase in three different models in the rat. *Neurosurgery* 2004; 54: 426–436.
5. Ostergaard L, Engedal TS, Aamand R, et al. Capillary transit time heterogeneity and flow-metabolism coupling after traumatic brain injury. *J Cereb Blood Flow Metab* 2014; 34: 1585–1598.
6. Agarwal S, Sair HI, Yahyavi-Firouz-Abadi N, et al. Neurovascular uncoupling in resting state fMRI demonstrated in patients with primary brain gliomas. *J Magn Reson Imaging* 2016; 43: 620–626.
7. Longden TA, Hill-Eubanks DC and Nelson MT. Ion channel networks in the control of cerebral blood flow. *J Cereb Blood Flow Metab* 2016; 36: 492–512.
8. McCarron JG and Halpern W. Potassium dilates rat cerebral arteries by two independent mechanisms. *Am J Physiol* 1990; 259: H902–H908.
9. Knot HJ, Zimmermann PA and Nelson MT. Extracellular K^+ -induced hyperpolarizations and dilations of rat coronary and cerebral arteries involve inward rectifier K^+ channels. *J Physiol* 1996; 492(Pt 2): 419–430.
10. Longden TA, Dabertrand F, Koide M, et al. Capillary K^+ -sensing initiates retrograde hyperpolarization to increase local cerebral blood flow. *Nat Neurosci* 2017; 20: 717–726.
11. Aziz Q, Thomas AM, Gomes J, et al. The ATP-sensitive potassium channel subunit, $K_{ir6.1}$, in vascular smooth muscle plays a major role in blood pressure control. *Hypertension* 2014; 64: 523–529.
12. Jansen-Olesen I, Mortensen CH, El-Bariaki N, et al. Characterization of K_{ATP} -channels in rat basilar and middle cerebral arteries: studies of vasomotor responses and mRNA expression. *Eur J Pharmacol* 2005; 523: 109–118.
13. Bondjers C, He L, Takemoto M, et al. Microarray analysis of blood microvessels from PDGF-B and PDGF-Rbeta mutant mice identifies novel markers for brain pericytes. *FASEB J* 2006; 20: 1703–1705.
14. Hall CN, Reynell C, Gesslein B, et al. Capillary pericytes regulate cerebral blood flow in health and disease. *Nature* 2014; 508: 55–60.
15. Mishra A, Reynolds JP, Chen Y, et al. Astrocytes mediate neurovascular signaling to capillary pericytes but not to arterioles. *Nat Neurosci* 2016; 19: 1619–1627.
16. Hill RA, Tong L, Yuan P, et al. Regional blood flow in the normal and ischemic brain is controlled by arteriolar smooth muscle cell contractility and not by capillary pericytes. *Neuron* 2015; 87: 95–110.
17. Attwell D, Mishra A, Hall CN, et al. What is a pericyte? *J Cereb Blood Flow Metab* 2016; 36: 451–455.
18. Li Q and Puro DG. Adenosine activates ATP-sensitive K^+ currents in pericytes of rat retinal microvessels: role of A1 and A2a receptors. *Brain Res* 2001; 907: 93–99.
19. Wells JA, Christie IN, Hosford PS, et al. A critical role for purinergic signalling in the mechanisms underlying generation of BOLD fMRI responses. *J Neurosci* 2015; 35: 5284–5292.
20. Niranjana A, Christie IN, Solomon SG, et al. fMRI mapping of the visual system in the mouse brain with

- interleaved snapshot GE-EPI. *Neuroimage* 2016; 139: 337–345.
21. Ourselin S, Roche A, Prima S, et al. In: International conference on medical image computing and computer-assisted intervention – MICCAI (eds SL Delp, AM DiGoia and B Jaramaz), **■■■■** 2000, Vol. 1935, pp. **■■■■**: Springer, 2000 **[AQ3]**.
 22. Penny WD, Friston KJ, Ashburner JT, et al. *Statistical parametric mapping: the analysis of functional brain images: the analysis of functional brain images*. **[AQ4]** **■■■■**: Academic Press, 2011.
 23. Lein ES, Hawrylycz MJ, Ao N, et al. Genome-wide atlas of gene expression in the adult mouse brain. *Nature* 2007; 445: 168–176.
 24. Paxinos G and Franklin KB. *The mouse brain in stereotaxic coordinates*. **[AQ5]** **■■■■**: Gulf Professional Publishing, 2004.
 25. Wang X, Wu J, Li L, et al. Hypercapnic acidosis activates K_{ATP} channels in vascular smooth muscles. *Circ Res* 2003; 92: 1225–1232.
 26. Nichols CG. K_{ATP} channels as molecular sensors of cellular metabolism. *Nature* 2006; 440: 470–476.
 27. Wells JA, Holmes HE, O’Callaghan JM, et al. Increased cerebral vascular reactivity in the tau expressing rTg4510 mouse: evidence against the role of tau pathology to impair vascular health in Alzheimer’s disease. *J Cereb Blood Flow Metab* 2015; 35: 359–362.
 28. Gozalov A, Petersen KA, Mortensen C, et al. Role of K_{ATP} channels in the regulation of rat dura and pia artery diameter. *Cephalalgia* 2005; 25: 249–260.
 29. Syed AU, Koide M, Brayden JE, et al. Tonic regulation of middle meningeal artery diameter by ATP-sensitive potassium channels. *J Cereb Blood Flow Metab* 2018; **■■■■** **[AQ6]**.
 30. Angelova PR, Kasymov V, Christie I, et al. Functional oxygen sensitivity of astrocytes. *J Neurosci* 2015; 35: 10460–10473.
 31. Marina N, Ang R, Machhada A, et al. Brainstem hypoxia contributes to the development of hypertension in the spontaneously hypertensive rat. *Hypertension* 2015; 65: 775–783.